

# Nonequilibrium Thermal Radiation from Air Shock Layers Modeled with Direct Simulation Monte Carlo

M. A. Gallis\* and J. K. Harvey†

*Imperial College of Science, Technology and Medicine, London SW7 2BY, England, United Kingdom*

At re-entry velocities it is generally agreed that the radiation associated with transitions between excited electronic states of atoms and molecules is responsible for the bulk of the thermal radiation emitted from the shock wave area. This article deals with the evaluation of thermal radiation emitted from hypersonic shock waves in real air using the direct simulation Monte Carlo method. The calculation of electronic excitation is made without assuming equilibrium for the distribution of the energy states, and measured or theoretically evaluated cross sections are used to determine the electronic excitation of atoms and molecules in the flow and the subsequent thermal radiation. The results with this new scheme are compared with available experimental data and existing numerical methods. The test cases are based on an AVCO Everett shock-tube experiment and on the axisymmetric flowfield of a blunted Mars-net re-entry vehicle. The method is in good agreement with both experimental data and results given by other methods. Discrepancies are evaluated and discussed.

## I. Introduction

THE ionization of the flow during hypersonic flight at high altitudes leads to the electronic excitation of the particles in the flow. It is generally agreed that for these flows collisions of heavy particles with electrons are mainly responsible for electronic excitation. So far, other radiation mechanisms such as atom-atom excitation and bremsstrahlung that are usually less important have not been included in the study. De-excitation of these excited states takes place either through collisions with other atoms or molecules, or by spontaneous emission of radiation following the law of natural decay of the excited states.

Emitted photons have different wavelengths depending on which mode their energy comes from (vibrational, rotational, electronic excitation). The spacing of the electronic states is usually several eV (especially of the low-lying electronic states). Radiative transitions from these states result in photons emitted or absorbed in the visible and uv region of the spectrum.

## II. Excitation by Electron Impact

During a collision between an electron and a heavy particle, energy from the electron or from the vibrational, rotational, or translational degrees of freedom (DOF) of the particle may be converted to electronic excitation energy with varying degrees of efficiency. Usually the change in the vibrational or rotational energy due to electron collisions is small since the excitation involves only a small number of closely spaced energy levels.

Electrons can be very effective in transferring kinetic energy to one of the orbiting electrons of the particles (by Coulomb forces), exciting it to a higher energy state (direct excitation). This is not the only excitation mechanism. Substitution of the orbiting electron by a higher energy free electron may take place, thereby exciting the particle (exchange excitation).

Radiation can also be absorbed by the flow giving rise to secondary phenomena. The secondary effects can be stimu-

lated emission of radiation by photon impact on excited particles, bremsstrahlung, or the production of an electron-positron pair. In the case of spacecraft rarefied flows the intensity of the total emitted radiation is generally small and reabsorption in the flow is not very significant, so that the secondary effects of radiative energy transfer within the flow can be ignored. Radiation heat transfer to the body surface may be measurable in some instances, but it has not been included in the present study.

## III. Electronic Excitation of Air Species

In this study real air is modeled with 11 species ( $N_2$ ,  $O_2$ ,  $N$ ,  $O$ ,  $NO$ ,  $N_2^+$ ,  $O_2^+$ ,  $N^+$ ,  $O^+$ ,  $NO^+$ ,  $e^-$ ). The six species that can be electronically excited and therefore radiate are  $N_2$ ,  $O_2$ ,  $NO$ ,  $N$ ,  $O$ , and  $N_2^+$ . These are not the only species that may radiate. Soon and Kunc<sup>1</sup> investigated the radiation from negative ions of atomic nitrogen and oxygen ( $O^-$ ,  $N^-$ ) and concluded that the radiation from these species is negligible under typical conditions met in aerospace applications.

For the four molecular species Bird<sup>2</sup> has proposed a radiation set with the states that are most likely to be excited. Electronic excitation is considered only for these states since the electronic excitation probability of the other states is significantly lower.

The number of electronic states for the atomic species is very large, and so we have to group them together. According to Bird,<sup>2</sup> eight main groups of states are considered for atomic oxygen and atomic nitrogen. This grouping is not unique. Park,<sup>3</sup> Kunc and Soon<sup>4,5</sup> have proposed different grouping of states for the atomic species. For this study the electronic states considered by Bird were adopted for the molecular and atomic species.

The probability of electronic excitation resulting from a collision can be calculated with the aid of electronic excitation cross sections. We can determine if electronic excitation will take place if we know the probability of an encounter resulting in the excitation. The electronic excitation probability in general depends on the species, the available energy, the states between which the transition takes place, and on the energy configuration of the particle (vibrational and rotational energy state).

Accurate measurements of the electron impact excitation cross sections are very difficult to make. Therefore, in many cases we have to resort to theoretical calculations of the cross sections, and in cases where these are difficult to derive we have to assume that they can be approximated by other known

Received Oct. 12, 1993; presented as Paper 94-0353 at the AIAA 32nd Aerospace Sciences Meeting, Reno, NV, Jan. 10–13, 1994; revision received March 30, 1994; accepted for publication April 15, 1994. Copyright © 1994 by the American Institute of Aeronautics and Astronautics, Inc. All rights reserved.

\*Research Associate, Department of Aeronautics. Member AIAA.

†Professor of Gas Dynamics, Department of Aeronautics. Member AIAA.

cross sections for similar interactions. This assumption is not an uncommon practice in this field.<sup>2,3</sup>

#### IV. Electron Impact Electronic Excitation of Atoms

Experimental data that are available for the electron impact electronic excitation of atoms cover transitions from the ground state only. In addition to these, several quantum mechanical, classical, and semi-empirical methods to calculate the cross sections have been proposed that in general are in good agreement with experimental data.

##### A. Phenomenological Cross Sections

Let us consider an electron, of energy  $E$ , performing an electronic excitation from state  $i$  to state  $j$ . The corresponding energy change is from  $E_i$  to energy  $E_j$ . The excitation cross section  $\sigma$  can be expressed as<sup>6</sup>

$$\sigma(E_j) = \frac{\pi a_0^2 (2R_e)^2 f_0}{E_j^2} g(\varepsilon) \quad (1)$$

where  $\varepsilon = E/(E_j - E_i)$ ,  $a_0$  is the Bohr radius,  $2R_e = 7.21$  eV is the atomic unit of energy, and  $f_0$  is the optical oscillator strength for the transition  $i \rightarrow j$ .  $g(\varepsilon)$  is a function of the electron energy and characterizes the dependence of the cross section on energy.

It has been observed<sup>6</sup> that the cross sections for excitation from the ground state rise from zero at threshold according to some power law, reach a peak, and then drop following a functional form of the type  $\propto (\varepsilon)/\varepsilon$  suggested by the Bohr approximation. The function  $g(\varepsilon)$  in Eq. (1) should account for this behavior. The values of this formula ideally come from experiment, but there are several empirical formulas available. A simple function that represents this behavior is

$$g(\varepsilon) = c_0 [1 - (1/\varepsilon)]^\nu \varepsilon^{-\omega} \quad (2)$$

According to Green<sup>6</sup> this functional form for  $g(\varepsilon)$  embodies the main characteristics of excitation cross sections from threshold ( $\varepsilon = 1$ ) to high energies ( $\varepsilon = 100$ ). The  $c_0$  parameter is preferably defined from experimental data, but in the absence of data Seaton's choice for  $\nu = 3$ ,  $\omega = 1.75$ , and  $c_0 = 1.5$ , is usually accepted.<sup>6</sup> Equation (1) offers a universal phenomenological formula for the electron impact cross section for allowed transitions. For forbidden transitions it has been observed<sup>7</sup> that the cross section falls off from the peak value as  $E^{-3}$  or  $E^{-2}$ . Therefore, these phenomenological formulas can be adjusted to cover the case of forbidden transitions as well. In the absence of experimental data for the magnitude of the forbidden cross sections the magnitude of the allowed transitions can be assumed to be representative.

##### B. Classical Excitation Cross Sections

Theoretical calculations for the electron impact excitation cross section have been made by Gryzinski,<sup>8,9</sup> Drawing,<sup>10</sup> and others. In the following, Gryzinski's approach will be outlined since it is the most extensive.

This approach deals with the interaction of the electrons of the two colliding bodies that leads to energy exchange. Since both interacting bodies are electrons, Gryzinski assumes Coulomb interaction between them. During the interaction the nuclear field around them is neglected.

The theory of binary inelastic Coulomb collisions is applied to calculate the cross sections without any arbitrary parameters. The calculation is made using the conservation of energy and momentum principles on simple approximate formulas without assuming anything for the velocity distribution of electrons.

The cross section for excitation to a state of energy  $E_j$  by an electron of energy  $E$ , is calculated as the cross section for a transition that will lead the target particle in the energy

range  $E_j - E_{j+1}$ . The cross section for a transition to a state  $j$  takes the form

$$\sigma = Q(E, E_j) - Q(E, E_{j+1}) \quad (3)$$

where

$$Q(E, E_j) = \frac{\sigma_0}{E_j^2} f \left[ \frac{E_j}{U_i} + \frac{2}{3} \left( 1 - \frac{E_j}{2U_i} \right) \right] \times \propto \left[ 2.7 + \left( \frac{E - E_j}{U_i} \right)^{1/2} \right] \left( 1 - \frac{E_j}{E} \right)^{1+|U_i/(U_i + E_j)|} \quad (4)$$

and the oscillator strength  $f$  is given by

$$f = \left( \frac{u_e}{u_i} \right)^2 \left( \frac{u_i^2}{u_i^2 + u_e^2} \right)^{3/2} \quad (5)$$

where  $U_i$  is the ionization potential, and  $u_i$  and  $u_e$  the ion and electron speed, respectively.

The calculation of the oscillator strength is the weakest point of the Gryzinski theory since deriving this is an intrinsically quantum mechanical project.

Gryzinski's approach has a considerable advantage over other methods. The calculation of the cross sections depends only on the energy range where the excited electron will find itself after the excitation. As mentioned in Sec. III, for practical reasoning it is common to treat electronic states in groups of states having different quantum numbers. The Gryzinski approach can be applied in this case as well.

##### C. Quantum Mechanical Methods for the Calculation of the Excitation Cross Section for Slow Electrons

At electron energies significantly lower than the excitation energy the assumptions made so far are no longer valid. The calculation of the cross section at these energies requires more elaborate analytical and computational procedures. There are several quantum mechanical computational methods to deal with this problem (e.g., variational method and distorted wave methods), which are reviewed by Massey<sup>7</sup> and Nesbet.<sup>11</sup>

All the methods that can deal with very low electron energies have been validated with experiments made mostly with hydrogen.<sup>7,12</sup> The results showed a general good agreement between the methods and the experiments.

Measurements of the excitation cross section of the first two first states of oxygen by slow electrons have been made by Doering and Shyn, which are reviewed in Soon and Kunc.<sup>4</sup> Computational methods that have been applied for the calculation of the cross sections for the excitation of the equivalent ground states of atomic nitrogen and oxygen<sup>11,12</sup> are in good agreement with measured cross sections.

##### D. Experimentally Measured Cross Sections for N and O

The majority of the measurements have been done on hydrogen to validate calculations of states of the same element. Measurements are available only for some of the states for the species of interest in aerochemistry. Stone and Zipf<sup>13,14</sup> have measured excitation cross sections for atomic oxygen and nitrogen. For nitrogen, measurements of cross sections for individual transitions have been made by Henry et al., which are reviewed by Kunc and Soon.<sup>5</sup> A thorough review of recent experimental data for oxygen can be found in Soon and Kunc.<sup>4</sup>

##### E. Comparison Between Electronic Excitation Models

Generally, all the computational methods presented above have been shown to yield results that are in good agreement with the experimental results. The various mathematical formalisms and the diversity of assumptions made for each of these methods make their critical evaluation very difficult.

Green<sup>15</sup> expressed all the cross sections with the aid of the phenomenological formula given by Eqs. (1) and (2). Green fitted his formula for the cross sections to most of those proposed by systematic theory formulas. He found that the parameters his formula needed to simulate any of the other formulas were similar.

The conclusion was that although these methods differ significantly in the assumptions made and in the methodology followed, all these studies lead to more or less the same result.

Bearing in mind that the results produced by each of those formulas are not expected to be very far from all the others, the question of determining the most appropriate computationally efficient method that can best fit the requirements of the specific application must be found among these results.

## V. Electron Impact Excitation of Molecules

Electrons colliding with molecules can be responsible for vibrational and rotational excitation of the target molecule, as well as electronic excitation. This further complicates the study of the excitation phenomenon and, hence, the theoretical calculations of the cross sections.

### A. Theoretical Evaluation of Electronic Excitation for Molecules

To overcome the difficulties of developing theoretical methods that will include all the phenomena associated with electronic excitation of molecules, a first approximation can be made by extending the theoretical approaches developed for atoms. The phenomenological formula that was presented in Sec. IV.A can be extended to the calculation of cross sections for molecules as well as atoms. As was concluded in the same paragraph, this formula seems to express a universal principle and it can easily be fitted to match most of the observed cross section behavior. The only input this formula requires is the energy of the final state and the oscillator strength. The oscillator strength has to be experimentally determined.

Huo and McKoy<sup>16</sup> have applied Schwinger's multichannel formulation to calculate the cross sections for molecular nitrogen. The calculation was extended to low energies for a number of vibrational and rotational temperatures, and the comparison with experimental results showed good agreement. This theory has not yet been applied to other species of interest.

Due to the difficulty in developing a reliable theoretical approach to cover all the cases of molecular electronic excitation, measurements have been made to determine the cross sections.

### B. Experimentally Measured Cross Sections for Molecular Species

**Nitrogen ( $N_2$ ):** The latest available and most complete measurements for the cross section of nitrogen are the ones by Cartwright et al.<sup>17</sup> In the actual experiment the differential cross sections were measured. The integral cross sections were obtained by numerical integration of the experimental data. The data for the integral cross section covers the area from 7 to 50 eV.

**Oxygen ( $O_2$ ):** The latest available and most complete measurements for the electronic excitation cross sections of oxygen are the ones by Wakiya.<sup>18</sup> Both differential and integral cross sections were measured for the ground vibrational states. The overall uncertainty in the cross sections for energies below 40 eV was defined as 40%. For the fifth state of  $O_2$  where no measurements are available, we have the oscillator strength as proposed by Allen<sup>19</sup> with  $f = 0.075$ .

**Molecular nitrogen ion ( $N_2^+$ ):** Cross sections of the molecular nitrogen ion are available only for the first negative system of  $N_2^+$ . This band is a strong radiator in nearly all plasmas containing nitrogen. For this reason all the effort has been focused in defining the cross section for this band. Measurements have been reported by Crandall et al.<sup>20</sup> Theoretical calculations for the first negative system have also been made by Seaton (see Ref. 21).

The results obtained for  $N_2^+$  from all of the sources mentioned have given a spectrum of cross sections that differ in some cases by as much as 2 orders of magnitude. The set of data obtained by Crandall et al. is in good agreement with Seaton's phenomenological formula.

**Nitric oxide (NO):** Experimental difficulties due to the characteristics of NO and the fact that the cross sections for the transitions of interest are rather small has resulted in a limited set of experimental data for this gas. Measurements have been made by Imami et al.<sup>22</sup> The measurements by Imami et al. give the cross sections for the gamma band of NO for a number of vibrational energy configurations. One can only resort to calculating the cross sections for all five bands of NO from Seaton's phenomenological cross-sectional formula. The oscillator strength for the NO bands can be obtained from measurements or theoretical calculations.<sup>6</sup>

## VI. Calculation of Electronic Excitation and Thermal Radiation with DSMC

A way to introduce the calculation of radiation into the DSMC calculations was demonstrated by Bird with his phenomenological method. In the context of DSMC calculations the electronic excitation problem is a mere case of energy exchange. It is important therefore to make sure that the assumptions made for electronic excitation are consistent with those made for energy exchange.

According to Bird's method,<sup>2,23</sup> for a specified fraction of the collisions for each species, the electronic states are sampled from an equilibrium distribution. Although the assumption of an equilibrium distribution of the electronic states is consistent with the Borgnakke and Larsen model almost universally used in the DSMC simulations for internal energy exchange, it is not physically realistic for flows where radiation is produced, since in the area of the shock wave and possibly elsewhere, the flow may well be in state of significant thermal nonequilibrium.

To simplify the excitation model, Bird assumed that the excitation rates are constant for each species for all electron energies. The fractions were chosen after numerical experiments to match experimental data.

Since the data available on radiation absorption by air species is rather incomplete, Bird adopted an approximate method for the calculation of the absorption probability in one-dimensional cases. If  $N_a$  is the number density of the absorbing particles in a cell of width  $x$ , the probability of absorbing a photon moving at an angle  $\theta$  to the axis of the cell is

$$P_{\text{absorption}} = [xN_a\sigma_a/\cos(\theta)] \quad (6)$$

Each time a photon is emitted, an angle  $\theta$  is chosen such that all directions in a cell are equally probable. The absorption probability is calculated using an accept-reject technique and the photon is absorbed or released. Carlson<sup>24</sup> argued that the only information needed to make Bird's approach physically realistic was the electronic relaxation numbers that are species and temperature dependent. Having reliable relaxation numbers the excitation probability could be accurately calculated, and it should not matter whether each particle is assigned a distribution of states or a single state. As a result an overestimation of the particle's electronic energy should not occur. To define the relaxation numbers Carlson used Park's<sup>3</sup> data for the electronic excitation rates. The distribution of energy is done according to Bird's scheme, where each excited particle is given the whole distribution of energy.

## VII. Approach Employed

Although the methods outlined in Sec. VI have produced very realistic results, their validity in the highly nonequilibrium region must be questioned, since the electronic excitation energy of a particle is taken from an equilibrium distribution. An outcome of assuming a distribution of the electronic

states is that a greater sample is gathered at the end of the simulation, which reduces the numerical noise. Bird himself suggested that such an option leads to a higher average electronic excitation energy than the real flow should have had under the same conditions. As it concerns the selection of an equilibrium distribution, no theoretical or experimental evidence that this assumption is physically realistic has been offered by Bird or Carlson.

In view of this criticism it was concluded that the idea of taking the energy from a distribution should be abandoned. Having the excitation cross section for each state the excitation probability after each collision can be calculated. A successful event would mean that the particle is excited to the energy of the state in question. It may be argued that this option may require a very large number of particles to obtain a satisfactory sample for each state, but in the simulations that were done (presented in Sec. VIII) the number of particles did not seem to play an important role for most of the species.

The problem of defining the correct excitation rate or the correct excitation cross section remains the most significant problem. From the review in Sec. VI we concluded that none of the available theoretical approaches and experimental measurements are able to give a totally reliable description of the excitation rates for all cases. All the theories that describe the electron impact excitation procedures are usually accurate to within a factor of about two or three. In contrast with the diversity of assumptions adopted and methods used, for the case of atomic species most of the theoretical approaches are in good agreement with each other, as Green<sup>15</sup> proved.

As a first approximation, and until further and more comprehensive theories or detailed experimental data are available, we will have to use the best of the existing data. The assumptions that come with each method may vary. Their usage in this study does not aim at validating in depth any of these methods or measurements. It is just an attempt to demonstrate an ability to simulate real flows using measured or calculated cross sections.

#### A. Selection of Available Cross Section Used in this Study

**Atomic species:** The available experimental data for the electronic excitation of atoms is very limited, and can only be used to validate the theoretical approaches. Due to the grouping of atom electronic states that was done to make the simulation of atomic excitation possible, the states cannot be addressed with their quantum numbers. This almost excludes all the quantum mechanical approaches that could be used. The phenomenological formula that was presented in Sec. III can be used, but there is a lack of suitable and accurate input data (oscillator strength for the combined transition). This leaves us with the classical mechanical excitation formula of Gryzinski (see Sec. IV.B), which requires only the energy of the final state as input.

The groups of states include allowed and forbidden transitions. Since in all these cases the forbidden transitions are only a small fraction of the total, the formulas for the allowed transitions can be used. There is one exception. The first two states of atomic nitrogen and oxygen can only be excited from the ground state via forbidden transitions. For these transitions we have a number of theories that are in very good agreement among themselves and with experimental data. Nesbet's variational method was used here to calculate the cross sections for those states.<sup>11</sup> Alternatively, the exchange cross section formula by Gryzinski<sup>18,9</sup> could be used. In any case since these two states do not radiate, their influence is indirect and the selection of either is not expected to significantly affect the results.

In the case of atoms that are already electronically excited, the excitation energy is added to the electron energy, thus assuming that the excitation rate for the transition from  $i$  to  $j$  is independent of the initial state  $i$ .

**Molecular species:** In the case of molecular electronic excitation the theoretical prediction of the excitation cross section is more difficult due to the greater number of DOF. The simultaneous rearrangement of the rotational and vibrational energy modes makes the theoretical evaluation of the excitation probability very difficult. Since the impact of the electron collision on the vibrational and rotational energy of a molecule is rather small the contribution of these energy modes to the electronic excitation energy was ignored.

The measurements of the cross sections have been made for the ground vibrational state in all cases. With the use of the Frank-Condon factor we can define an average cross section over all the vibrational states. The Frank Condon factors for all the molecular species of interest have been given by Nicolls.<sup>25,26</sup>

For  $N_2$  the measurements of Cartwright (see Fig. 1), and for  $O_2$  the measurements of Imami were used. The fifth state of  $O_2$  where no measurements are available was approximated with Seaton's formula using the oscillator strength proposed by Allen.

For NO we have the oscillator strengths as calculated by Ory (see Ref. 15) for four of the transitions in question. The last state was assumed to have the same oscillator strength as the fourth state. These oscillator strengths can be used with Seaton's phenomenological formula to give the cross sections for NO (see Fig. 2). In Fig. 2 the cross section for the second state based on Imami's measurements is shown for comparison.

For  $N_2^+$  we have the measurement of Crandall for the second state. For the first and third state of  $N_2^+$  no measurements

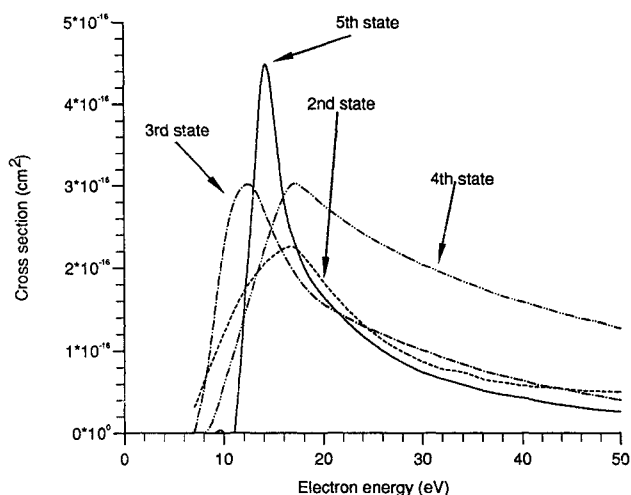


Fig. 1  $N_2$  electronic excitation cross sections.

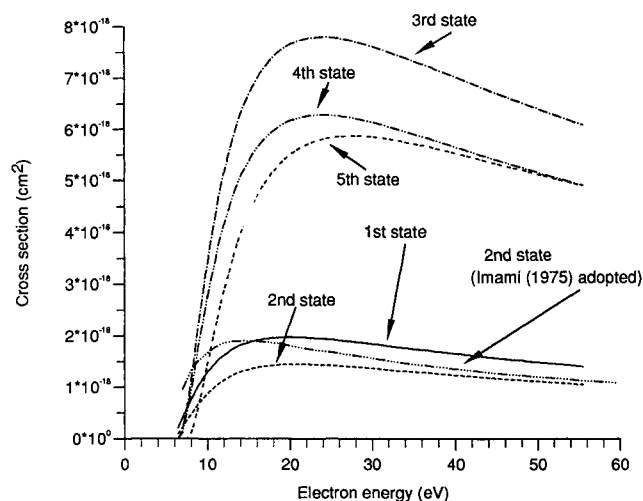


Fig. 2 NO electronic excitation cross sections.

are available and we have to resort to the phenomenological formula. For the first state we have the oscillator strength proposed by Allen.<sup>19</sup> For the third state of  $N_2^+$  we assumed that the oscillator strength was equal to the oscillator strength for the second. In the light of the uncertainty for the order of magnitude of the measured cross sections, the formula of Seaton [Eq. (2)] can be considered to give the most reliable results.

### B. Absorption of Emitted Radiation

Experimental study (i.e., Refs. 12 and 27) of the absorption cross sections of atmospheric molecular species have shown that for the wavelengths of interest (the range is  $0.1\text{--}10\ \mu\text{m}$ ), the absorption cross sections are of the order of  $10^{-18}\ \text{cm}^2$ .

In contrast, the contributions to absorption of the atomic species (N and O) are the most significant both due to their large cross section and because the atomic species comprise the bulk of the flow in the downstream area. The maximum absorption cross sections for both N and O were measured<sup>28,29</sup> to be of the order of  $10^{-17}\ \text{cm}^2$ .

In high altitude rarefied flows the fraction of the emitted radiation that is absorbed by the flow is not very large. Since the whole approach applied in this study for the calculation of the emitted radiation was approximate in nature, Bird's approximate approach for the absorbed radiation was adopted. When a photon is emitted, the probability of it being absorbed is calculated within the cell from which it was emitted. In this cell the atomic species are assumed to be absorbing with their maximum cross section over all wavelengths. The absorption cross section of N and O was assumed to be  $4 \times 10^{-17}\ \text{cm}^2$ . If a photon is absorbed its effect is totally ignored. This violates conservation of energy and the procedure cannot be used if significant energy is absorbed.

## VIII. Computational Results and Comparison with Experiment

As a test case to validate the model developed, the conditions of a shock-tube experiment<sup>30</sup> were used. In this experiment the spectral radiation emission from the equilibrium and nonequilibrium region of the shock layer in air were measured. The experiment was made with air (79%  $N_2$ , 21%  $O_2$ ) at Mach 29 and pressure 0.1 Torr.

For the simulation of the energy exchange and chemical and ionizing reactions in the flowfield, the maximum entropy method<sup>31</sup> was used. Eleven species were considered for the simulation of real air, i.e.,  $N_2$ ,  $O_2$ , N, O, NO,  $N_2^+$ ,  $O_2^+$ ,  $N^+$ ,  $O^+$ , NO<sup>+</sup>,  $e^-$ . For the simulation, 300,000 particles were used in a grid of 1000 cells. 120,000 time steps were executed. Steady state was reached at 55,000 time steps and the flowfield was sampled from 60,000 to 120,000 time steps. Tests performed with only 100,000 particles and 100 cells showed sim-

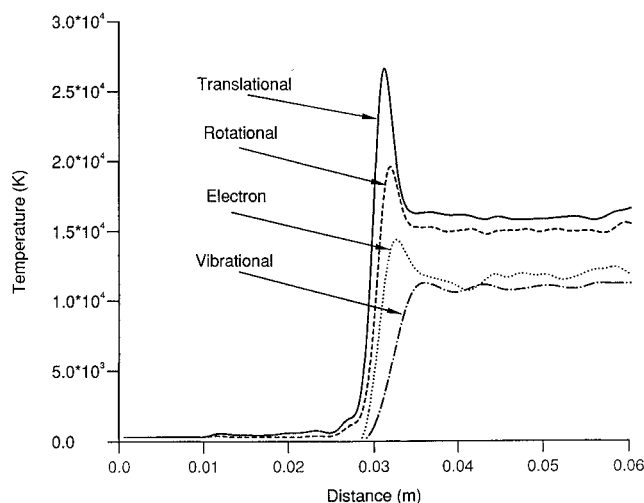


Fig. 3 Temperature profiles for air Mach 29 shock wave.

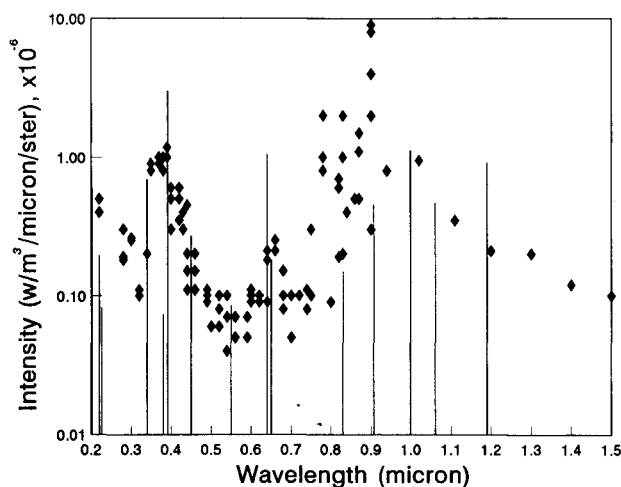


Fig. 4 Equilibrium spectral intensity for air Mach 29 shock wave.

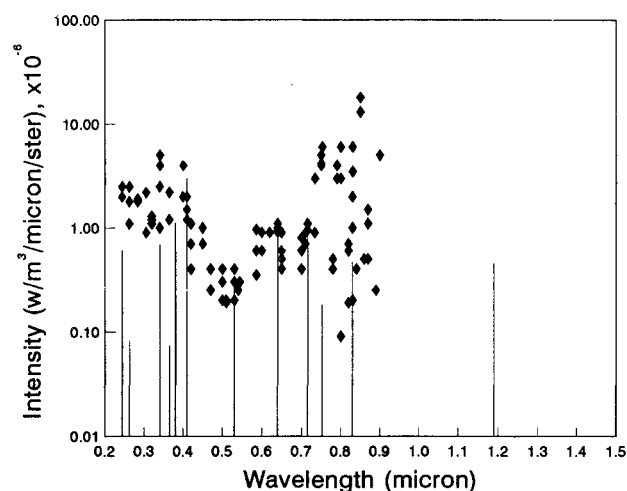


Fig. 5 Nonequilibrium spectral intensity for air Mach 29 shock wave.

ilar results and, hence, it is concluded that there is no cell or particle number dependence in the presented results. The temperature profiles for this case are presented in Fig. 3. The length behind the shock wave corresponds to only  $10^{-6}$  s of real time, and as a result the flow did not have the time to reach equilibrium. Similar results showing the same behavior have been presented by Park.<sup>3</sup> The electron temperature was calculated using the electron flux method.<sup>32</sup> In the equilibrium region the degree of ionization was found to be 2.7%.

Allen's measurements for the spectral radiation are presented in Figs. 4 and 5 for the equilibrium and nonequilibrium region, respectively, with solid diamonds. The predictions of the DSMC code used in this study are presented in the same figures with vertical lines. For this simulation the equilibrium region was estimated to occupy the last 75% of the flowfield. Close examination of these figures shows a rather encouraging agreement for most frequencies with the experimental data. There are two wavelengths (0.64 and  $0.83\ \mu$ ) where the agreement is not good. The 0.64 wavelength is overestimated and the 0.83 is underestimated. Both wavelengths belong to atomic oxygen. There is no special reason why the same approach that seems to predict the nitrogen frequencies should fail for oxygen.

The prediction for the equilibrium region seems to be in good agreement with the experimental results, whereas the spectral intensities due to atomic species in the nonequilibrium region (Fig. 5) seem to be underestimated. At the same time the wavelengths that are overestimated in the equilibrium region seem to be in better agreement in the nonequilibrium region. This shift to lower energies could be due to an overestimation of the absorption coefficient in the non-

Table 1 Flight conditions for "Mars-net" capsule

| Altitude, km | Speed, km/s | $T_{\text{wall}}$ , K | $T_{\infty}$ , K | $Kn$                 | Number density, $\text{m}^{-3}$ |
|--------------|-------------|-----------------------|------------------|----------------------|---------------------------------|
| 70           | 10          | 1000                  | 219.585          | $3.6 \times 10^{-4}$ | $1.72 \times 10^{21}$           |
| 80           | 12          | 1500                  | 198.639          | $1.5 \times 10^{-3}$ | $3.80 \times 10^{20}$           |

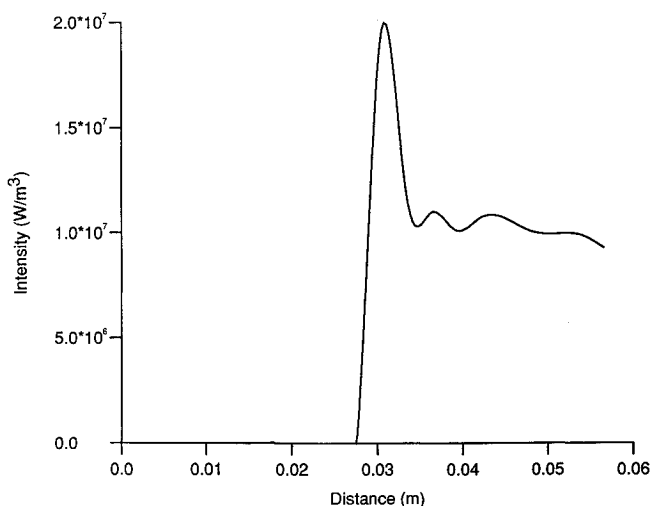


Fig. 6 Total radiation intensity for air Mach 29 shock wave.

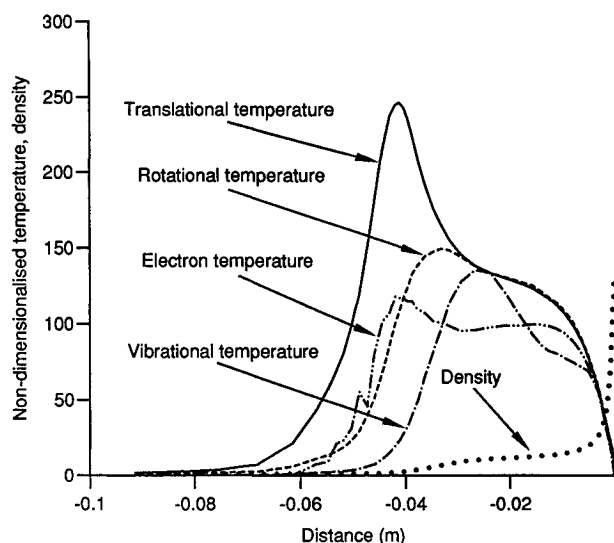


Fig. 7 Mars-net body temperature and density profiles along the stagnation streamline for air at 12 km/s.

equilibrium region and the concentration of the radiating species (N, O) in the nonequilibrium region of the computational flowfield being low and, hence, the statistical sample may not be large enough to reflect the actual radiation intensities.

It should be noted that Carlson<sup>24</sup> using Park's<sup>3</sup> data had the same problem in those frequencies. Carlson's method appears to overestimate by one order of magnitude the contribution of  $N_2^+$ . No explanation has been given by Carlson for this discrepancy.

Bird's method was fitted in such a way that the method would predict as closely as possible this particular experiment. All the excitation probabilities that were presented in Sec. VI were fitted to this experimental data. Although his method was fitted to predict this experiment well, a few discrepancies were not avoided. According to the results that Bird has presented, the  $0.64\text{-}\mu$  wavelength seems to be underestimated. Since Bird's excitation cross sections are approximate no conclusions can be drawn from the behavior of his model at specific wavelengths.

Taking into consideration that the two codes (Carlson's and the present code) that predicted this behavior are using different models to simulate the electronic excitation, and assuming that the measurement is correct, it indicates that there is probably another radiating mechanism at these frequencies that has not been taken into consideration. There is possibly another species or state of the existing species that strongly radiates in the  $0.83\text{-}\mu$  frequency that has been omitted from the band model. The overestimation of the  $0.64\text{-}\mu$  wavelength suggests that the absorption at that frequency might be stronger than the rather approximate model is anticipating.

The total radiation emission from the shock wave was not measured in the experiment, but qualitative oscillograph records of the total emitted radiation were obtained. These oscillographs show that the radiation peaks in the nonequilibrium region, and then it drops exponentially.

From tables<sup>19,33</sup> giving the absolute intensity of radiation at various altitudes and velocities, we read that the equilibrium level of radiation for the conditions of the experiment should be  $10\text{ W/cm}^3$ .<sup>3</sup> From the oscillographs presented,<sup>30</sup> we conclude that the nonequilibrium radiation peak should be around 2–3 times the value of the equilibrium value.

The total radiation intensity as calculated from the DSMC code used in this study is presented in Fig. 6. The nonequilibrium peak value is almost  $20\text{ W/cm}^3$ , whereas the equilibrium value tends to  $10\text{ W/cm}^3$ .

Although some discrepancies have been observed in the spectral intensity distribution for both the equilibrium and nonequilibrium region, the total radiation seems to be in good agreement with the available data both qualitatively and quantitatively. For the same case Carlson predicted a peak nonequilibrium value of  $10\text{ W/cm}^3$  and Bird predicted  $0.1\text{ W/cm}^3$ .

Judging from the uncertainty of the cross section data the prediction of the spectral intensities as a first approximation can be considered as acceptable. It should be noted that the experimental data by Allen present significant scatter in some wavelengths and therefore cannot be used as definitive data.

As a second example of the use of the present DSMC scheme the radiation emission from the axisymmetric shock layer around Mars-net, a 60-deg, spherically blunted cone of base radius 1 m has been calculated. The ratio of the nose radius to the base radius of vehicles is 1.25. The shape of the vehicle is similar to the 60-deg re-entry type of vehicles studied by Mitcheltree and Gnoffo.<sup>34</sup> The flowfield has been studied for two cases. The conditions of the simulations are presented in Table 1. The Knudsen number has been calculated using the base radius of the cone, and the mean free path as it is calculated for VHS particles. The simulations were made over a grid of 2550 cells covering the front of the body only, with 750,000 particles. The simulation was made for 25,000 time steps, and steady state was reached after about 10,000. The temperature profiles along the stagnation streamline at 80 km are shown in Fig. 7. In this figure the density and the temperature have been nondimensionalized by their freestream values. It is interesting to note that in the area between  $x = -0.03$  and  $x = -0.005$  m, the vibrational temperature falls below the translational and rotational temperature. This is mainly due to the ionic reactions that take place in this area which, according to the ME method used, are controlled by the vibrational temperature. A second reason for it is the energy loss due to radiation from this area. The prominent characteristic of the radiation profiles is the very sharp radiation peak on the stagnation line. The radiation emission along the stagnation line rises and peaks very rapidly in the

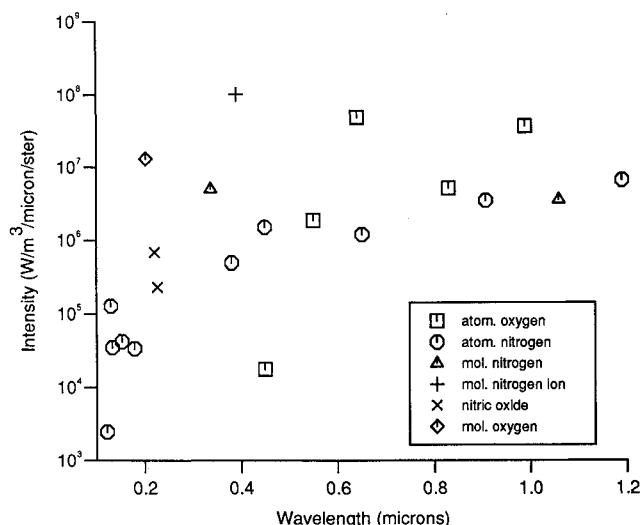


Fig. 8 Mars-net spectral intensity for air at 80 km and 12 km/s.

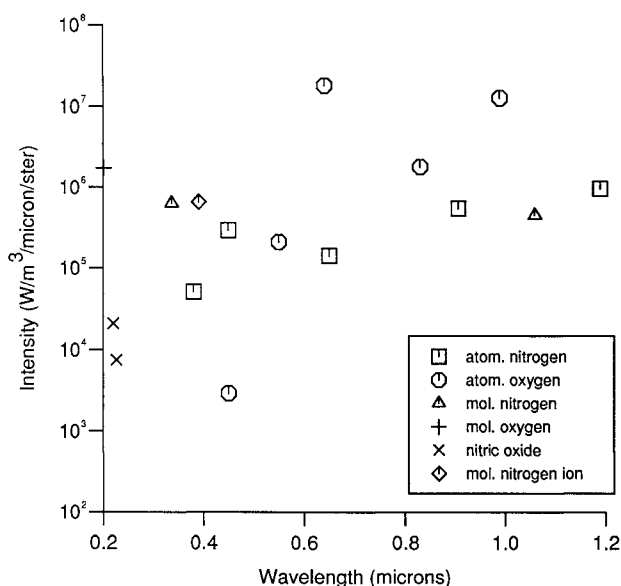


Fig. 9 Mars-net spectral intensity for air at 70 km and 10 km/s.

nonequilibrium area. The radiation peak coincides spatially with the temperature peak justifying its epithet as thermal radiation. The radiation peak falls very rapidly away from the stagnation streamline due to the expansion in the flow in the radial direction. As the temperature drops towards the body, the radiation emission also drops. The maximum value of radiation for the two cases in the nonequilibrium area was found to be  $1.65 \times 10^6$  and  $0.55 \times 10^6$  W/m<sup>3</sup> at 80 and 70 km, respectively. We note that radiation intensity follows closely the temperature of the flowfield.

Since radiation emission is significant only from a small area of the flow, and since the total energy radiated is a small fraction of the total energy, its effect on the flowfield is not expected to be large. Our assumption that the fraction of the radiated energy that is absorbed can be ignored without any significant error appears to be justified.

The total spectral radiation profiles for the whole flowfield are presented in Figs. 8 and 9, nearly all of which comes from the intense region close to the stagnation streamline. For the 80-km case, the contribution of N<sub>2</sub><sup>+</sup> was found to be the most significant. For the 70-km case, where the degree of ionization drops, the contribution of N<sub>2</sub><sup>+</sup> to the total radiation drops as well and the contribution of the atomic species is more pronounced.

## IX. Conclusions

The available experimental and theoretical data for the electronic excitation of atoms and molecules have been examined and a digested combination of them has been used for the prediction of the radiation emission from hypersonic rarefied shock waves. Comparison of the computational results with the experiment indicates encouraging agreement, therefore validating the argument that the prediction of electronic excitation can be made without any assumptions about the distribution of the electronic states.

## Acknowledgments

This work was supported by the British Ministry of Defence (D.R.A. Farnborough) under agreement AT/2037/331.

## References

- Soon, W. H., and Kunc, J. A., "Nitrogen-Plasma Continuum Emission Associated with N<sup>+</sup>(<sup>3</sup>P) and N<sup>+</sup>(<sup>1</sup>D) Ions," *Physical Review A*, Vol. 41, No. 8, 1990.
- Bird, G. A., "Non-Equilibrium Radiation During Re-Entry at 10 km/s," AIAA Paper 87-1543, June 1987.
- Park, C., *Non-Equilibrium Hypersonic Aerothermodynamics*, Wiley, New York, 1990.
- Soon, W. H., and Kunc, J. A., "Thermal Non-Equilibrium in Partially Ionised Atomic Oxygen," *Physical Review A*, Vol. 41, No. 2, 1990, pp. 825-845.
- Kunc, J. A., and Soon, W. H., "Collisional-Radiative Non-Equilibrium in Partially Ionised Atomic Nitrogen," *Physical Review A*, Vol. 40, No. 10, 1989, pp. 5822-5843.
- Green, A. E. S., *The Middle Ultraviolet: Its Science and Technology*, Wiley, New York, 1966.
- Massey, H. S. W., and Burhop, E. H. S., *Electronic and Ionic Impact Phenomena*, Oxford Univ. Press, London, 1969.
- Gryzinski, M., "Two Particle Collisions. I. General Relations for Collisions in the Laboratory System," *Physical Review*, Vol. 138, No. 2A, 1965, pp. 305-321.
- Gryzinski, M., "Two Particle Collisions. II. Coulomb Collisions in the Laboratory Frame of Reference," *Physical Review*, Vol. 138, No. 2A, 1965, pp. 322-335.
- Drawing, H. W., "Zur Formelmässigen Darstellung der Ionisierungsquerschnitte gegenüber Elektronstoss," *Zeitschrift fuer Physik*, 164, 513, 1961.
- Nesbet, R. K., *Variational Methods in Electron-Atom Scattering Theory*, Plenum Press, New York, 1980.
- Rees, M. H., "Physics and Chemistry of the Upper Atmosphere," Cambridge Atmospheric and Space Series, 1989.
- Stone, E. J., and Zipf, E. C., "Electron-Impact Excitation of the S and S States of Atomic Oxygen," *Journal of Chemical Physics*, Vol. 60, 1974, pp. 4237-4243.
- Stone, E. J., and Zipf, E. C., "Excitation of Atomic Nitrogen by Electron Impact," *Journal of Chemical Physics*, Vol. 58, 1973, pp. 4278-4284.
- Green, A. E. S., "Electron Cross Sections for Aeronomy," *AIAA Journal*, Vol. 4, No. 5, 1966, pp. 769-775.
- Huo, W. M., and McKoy, V., "The Production of Excited Molecular Species by Electron Impact in High Temperature Nonequilibrium Air," AIAA Paper 87-1634, June 1987.
- Cartwright, D. C., et al., "Electron Impact Excitation of the Electronic States of N<sub>2</sub>. Integral Cross Sections at Incident Energies from 10 to 50 eV," *Physical Review A*, Vol. 16, No. 3, 1977, pp. 1041-1051.
- Wakiya, K., "Differential and Integral Cross Sections for the Electron Impact of O<sub>2</sub>. II. Optically Forbidden Transitions from the Ground State," *Journal of Physics B. Atomic and Molecular Physics*, Vol. 11, No. 22, 1978, pp. 3931-3938.
- Allen, R. A., "Air Radiation Graphs: Spectrally Integrated Fluxes Including Line Contributions and Self Absorption," AVCO Everett Research Lab., Research Note 561, MA, July 1965.
- Crandall, D. H., and Kaupilla, W. E., "Absolute Cross Sections for Electron-Impact Excitation of N<sub>2</sub><sup>+</sup>," *Physical Review A*, Vol. 9, No. 6, 1974, pp. 2545-2551.
- Bates, D. R., *Atomic and Molecular Processes*, Academic Press, New York, 1962.
- Imami, M., and Borst, W. L., "Electron Impact Excitation of the Gamma Bands of Nitric Oxide," *Journal of Chemical Physics*, Vol. 63, No. 8, 1975, pp. 3602-3605.
- Bird, G. A., "Non-Equilibrium Thermal Radiation for an Aero-

assist Flight Experiment Vehicle," AIAA Paper 88-2205, July 1988.

<sup>24</sup>Carlson, A. B., and Hassan, H. A., "Radiation Modelling with Direct Simulation Monte Carlo," AIAA Paper 91-1409, June 1991.

<sup>25</sup>Nicholls, R. W., "Frank-Condon Factors to High Vibrational Quantum Numbers I:  $N_2$  and  $N_2^+$ ," *Journal of the National Bureau of Standards-A. Physics and Chemistry*, Vol. 68A, No. 5, 1964.

<sup>26</sup>Nicholls, R. W., "Frank-Condon Factors to High Vibrational Quantum Numbers IV: NO Bands Systems," *Journal of the National Bureau of Standards-A. Physics and Chemistry*, Vol. 68A, No. 5, 1964.

<sup>27</sup>Watanabe, K., "Ultraviolet Absorption Processes in the Upper Atmosphere," *Advances in Geophysics*, Vol. 5, 1958, pp. 153-221.

<sup>28</sup>Bates, D. R., and Seaton, M. J., "The Quantal Theory of Continuous Absorption of Radiation by Various Atoms in Their Ground States. II. Further Calculations in Nitrogen, Oxygen and Carbon," *Monthly Notices of the Royal Astronomical Society*, Vol. 109, 1949, pp. 698-704.

<sup>29</sup>Ehler, A. W., and Weissler, G. L., "Ultraviolet Absorption of Atomic Nitrogen in its Ionisation Continuum," *Journal of the Optical*

*Society*, Vol. 45, 1955, pp. 1035-1043.

<sup>30</sup>Allen, R. A., Rose, P. H., and Camm, J. C., "Nonequilibrium and Equilibrium Radiation at Super Satellite Re-Entry Velocities," AVCO Everett Research Lab., Research Rept. 156, Sept. 1962.

<sup>31</sup>Gallis, M. A., and Harvey, J. K., "Application of the Maximum Entropy Approach for the Prediction of Energy Exchange, Chemical and Ionising Reactions in the Direct Simulation Monte Carlo Method in Rarefied Hypersonic Flows," IC-AERO Rept. 93-01, ISSN 0308-7247, London, 1993.

<sup>32</sup>Gallis, M. A., "Simulation of Radiating Ionised Flows in the Rarefied Hypersonic Regime," Ph.D. Dissertation, Univ. of London, London, 1993.

<sup>33</sup>Camm, J. C., Kivel, B., Taylor, R. L., and Teave, J. D., "Absolute Intensity of Non-Equilibrium Radiation in Air and Stagnation Heating at High Altitudes," AVCO Everett Research Lab., Research Rept. 93, Sept. 1959.

<sup>34</sup>Mitcheltree, R. A., and Gnoffo, P. A., "Thermochemical Non-equilibrium Issues for Earth Re-Entry of Mars Mission Vehicles," *Journal of Spacecraft and Rockets*, Vol. 28, No. 5, 1991, pp. 552-559.